

Vibro-acoustic analysis of automotive air ducts using porous materials

Yoshio Kurosawa^{1,a,*}, Tsuyoshi Yamashita^{2,b}, Tetsuya Ozaki^{2,c},
Naoyuki Nakaizumi^{2,d}, Yuki Fujita^{2,e}, and Manabu Takahashi^{3,f}

¹Faculty of Science and Technology, Teikyo University, 1-1 Toyosatodai,
Utsunomiya City 320-8551, Japan

²Acoustic Research & Development Dept., Parker Corporation, 15 Kitane,
Fukaya City 369-1242, Japan

³Noise Control Materials and Technology Dept., Parker Asahi Co., Ltd., 15 Kitane,
Fukaya City 369-1242, Japan

*Corresponding author

^a<ykurosawa@mps.teiyo-u.ac.jp>, ^b<t-yamashita@parkercorp.co.jp>, ^c<ozaki@parkercorp.co.jp>,
^d<nakaizumi@parkercorp.co.jp>, ^e<y-fujita@parkercorp.co.jp>, ^f<takahashi-m@parker-asahi.co.jp>

Keywords: automotive air duct, porous media, biot-allard model, fem

Abstract. The electrification of automobiles has progressed in response to environmental problems. Accordingly, the number of automobiles equipped with large and large-capacity batteries, such as electric vehicles and hybrid vehicles, is increasing. These batteries take in air from the passenger compartment using ducts for cooling. However, since the cooling fan operates regardless of the running condition, sound may leak into the car interior through the ducts. To reduce such cabin noise, we examined the use of sound-absorbing ducts. We developed four types of test pieces using conventional polypropylene resin, compression felt, and film on the inside and outside of the compression felt. We measured the insertion loss in two ways: one on the opposite side and the other on the outside from the entrance of the duct. Acoustic attenuation was measured. The results of creating and calculating a similar FE model were then reported.

1. Introduction

The electrification of automobiles has progressed in response to environmental problems in recent years, resulting in the increasing number of automobiles equipped with large and large-capacity batteries, such as electric vehicles and hybrid vehicles. These batteries take in air from the passenger compartment using ducts for cooling, but since the cooling fan operates regardless of the running condition, sound may leak into the interior through the ducts. To reduce cabin noise, we investigate the use of sound-absorbing material for the ducts. H.J. Sabine obtained an approximate formula for calculating the amount of reduction in insertion loss when sound-absorbing material is attached to the entire inside surface of a resin duct [1]. L.L. Beranek sought a formula for calculating the insertion loss when sound-absorbing material is attached to part of the inside of a plastic duct [2]. The purpose of this research is to use an FE model to make it possible to predict the amount of noise reduction that can be achieved by making the material of the duct sound-absorbing in order to prevent the noise from the battery cooling fan in hybrid and electric vehicles from leaking into the vehicle through the duct. We developed four types of test pieces using conventional polypropylene (PP) resin, compressed felt, and film on both sides of the compressed felt. We measured the sound volume reduction on the opposite side and outside the entrance of the duct, and the acoustic performance was measured. The results of creating and calculating a similar FE model are described herein.

2. Analytical method

There are formulas for calculating the sound pressure inside a duct, assuming that the duct is a rigid body [1], [2]. In this research, the sound absorption of the felt used for the sound-absorbing duct was calculated using the Biot–Allard model [3], which handles the skeleton and internal air. In the Biot–Allard model, the incident sound entering the material is transmitted through the gaps of the porous elastic body (urethane, glass, wool, etc.) of the material, which is the air propagation sound, whereas the solid propagation sound is transmitted inside the material. This is a theoretical formula for predicting displacement. The displacement of the skeleton considering the interaction between the solid propagation and the air propagation sound: \vec{u}^s and the displacement of the fluid: \vec{u}^f are expressed as equations (1) and (2), respectively.

$$((1 - \phi)\rho_s + \rho_a)\frac{\partial^2 \vec{u}^s}{\partial t^2} - \rho_a \frac{\partial^2 \vec{u}^f}{\partial t^2} = (P - N)\vec{\nabla}(\vec{\nabla} \cdot \vec{u}^s) + Q\vec{\nabla}(\vec{\nabla} \cdot \vec{u}^f) + N\nabla^2 \vec{u}^s - \sigma\phi^2 G(\omega)\frac{\partial}{\partial t}(\vec{u}^s - \vec{u}^f) \quad (1)$$

$$(\phi\rho_f + \rho_a)\frac{\partial^2 \vec{u}^f}{\partial t^2} - \rho_a \frac{\partial^2 \vec{u}^s}{\partial t^2} = R\vec{\nabla}(\vec{\nabla} \cdot \vec{u}^f) + Q\vec{\nabla}(\vec{\nabla} \cdot \vec{u}^s) + \sigma\phi^2 G(\omega)\frac{\partial}{\partial t}(\vec{u}^s - \vec{u}^f) \quad (2)$$

ϕ : Porousness, ρ_s : Porous skeleton density, ρ_f : Fluid density (air in this paper), ρ_a : Equivalent density of fluid considering viscous decay in the interaction between skeleton and fluid. ρ_a is shown in Eq. (3).

$$\rho_a = \alpha_\infty \rho_f \left(1 + \frac{\phi\sigma}{j\omega\rho_f\alpha_\infty} \sqrt{1 + j\frac{4a_\infty^2\eta\rho_f\omega}{\sigma^2\Lambda^2\phi^2}} \right) \quad (3)$$

η : Solid loss coefficient, σ : Flow resistance, α_∞ : Maze degree, Λ : Viscous characteristic length. The elastic modulus P , Q , R is shown in Eq. (4).

$$P \approx \frac{4}{3}N + K_b + \frac{(1-\phi)^2}{\phi}K_f, \quad Q \approx (1-\phi)K_f, \quad R \approx \phi K_f \quad (4)$$

N : Skeleton shear modulus (in vacuum), K_b : Skeleton bulk modulus (in vacuum), K_f : Equivalent rigidity of fluid considering thermal decay in the interaction between skeleton and fluid. N , K_b , K_f are shown in Eq. (5).

$$N = \frac{E(1+j\eta)}{2(1+\nu)}, \quad K_b = \frac{2(1+\nu)}{3(1-2\nu)}N, \quad K_f = \frac{\gamma P_0}{\gamma - (\gamma - 1) \left[1 + \frac{8\zeta}{j\omega\Lambda'^2} \sqrt{1 + \frac{j\omega\Lambda'^2}{16\zeta}} \right]^{-1}} \quad (5)$$

γ : Specific heat ratio, P_0 : Equilibrium pressure, ζ : Thermal diffusivity, Λ' : Thermal characteristic length.

3. Experimental results and FE analysis results

3.1 Experimental results

Figure 1 shows the dimensions and layout of the duct test piece created for this experiment. The duct shape was simplified to a rectangular parallel pipe with internal dimensions of 85 mm × 15 mm

× 500 mm. A volume velocity speaker was used as the sound source in the anechoic chamber, and the sound pressure level was measured using three microphones (“Mic” in the figure). Mic3 was installed at a position 30 mm away from the surface, and two types of volume reduction (Mic1–Mic2 and Mic1–Mic3) were measured. Volume reduction (dB) indicates that the larger the value, the quieter the sound.

Figure 2 shows the results of volume reduction measurement. Four types of values for each 1/3 octave band from 200 Hz to 10000 Hz (compressed felt with a thickness of 2 mm; a test piece with a film attached to the outside of the compressed felt; a test piece with films attached to both sides of the compressed felt; and a PP resin test piece) were used for comparison. At the entrance–exit (Mic1–Mic2) of the duct, the compression felt type performed best up to 2500 Hz, whereas the type with a film on the outside performed best above 2500 Hz. These findings indicate the effect of sound absorption in the duct. Near the center of the duct entrance–outside (Mic1–Mic3), the difference was small among the four specifications compared with that for the duct inlet–outlet. However, the type with the film on the outside was slightly better than the conventional resin type. These findings suggest the effect of sound absorption and sound insulation of the duct material.

The test piece shown this time is a test piece with both the sound source side and the outlet side covered with rubber. However, the results when the outlet side is not closed did not vary significantly from those when the exit side was closed.

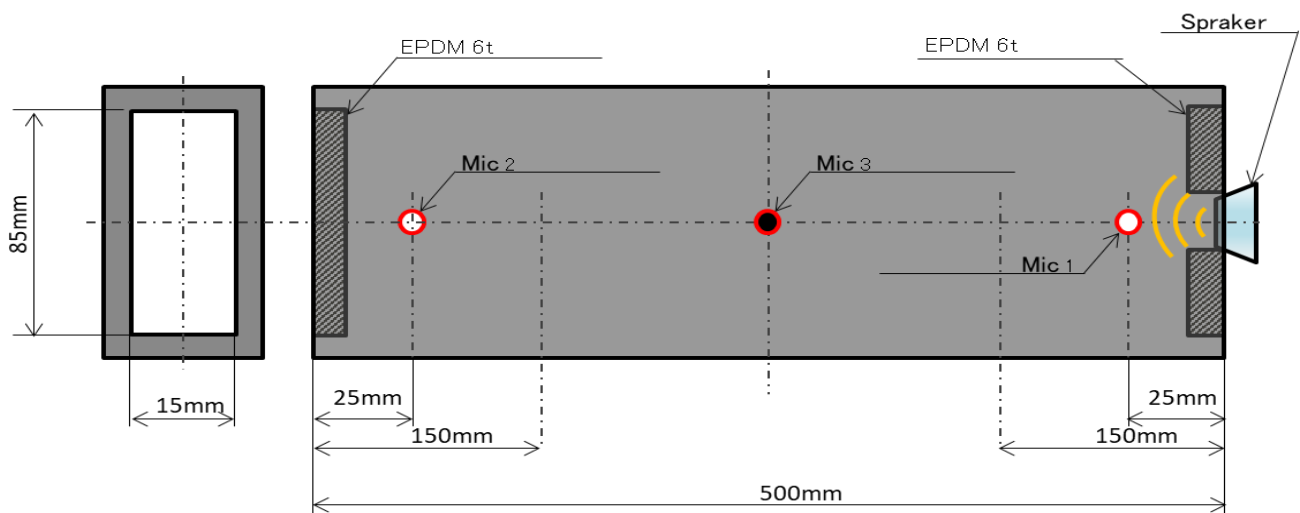


Fig. 1. Dimensions of the test piece duct and experimental setup.

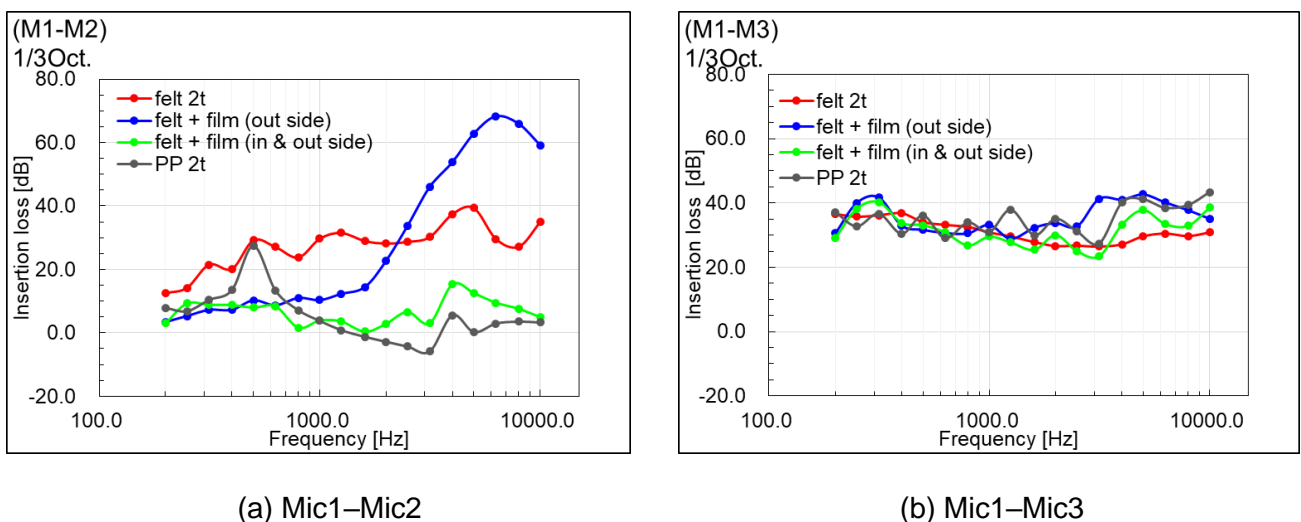


Fig. 2. Comparison of four types of insertion loss.

3.2 Comparisons of experimental and calculated results

Figure 3 shows the FE model for acoustic analysis of the duct. A hemispherical space was created around the sound source, and the spherical surface was set to non-reflective conditions. The volume velocity measured during the experiment was used as the input value. The sound pressure level was calculated at the same measurement position as in the experiment to measure the volume reduction. Figures 4–7 show comparisons of the experimental and calculation results of the four types of volume reduction. The calculated results were able to roughly reproduce the experimental results.

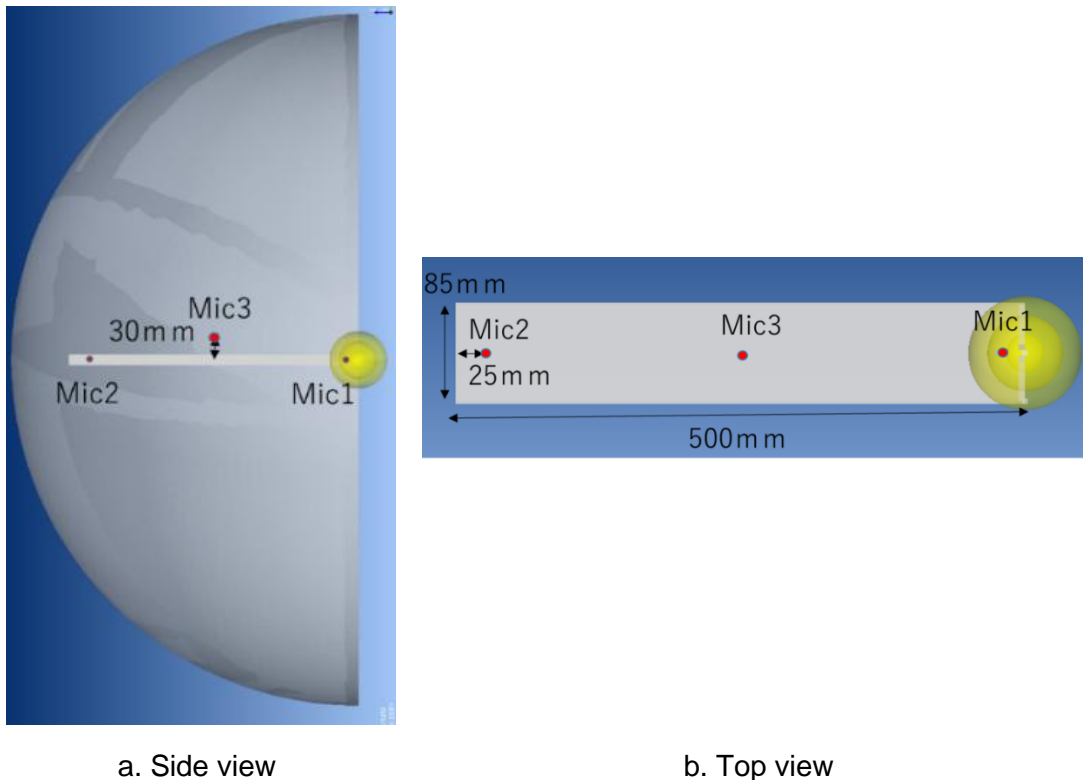


Fig. 3. FE model of duct and acoustic space (air).

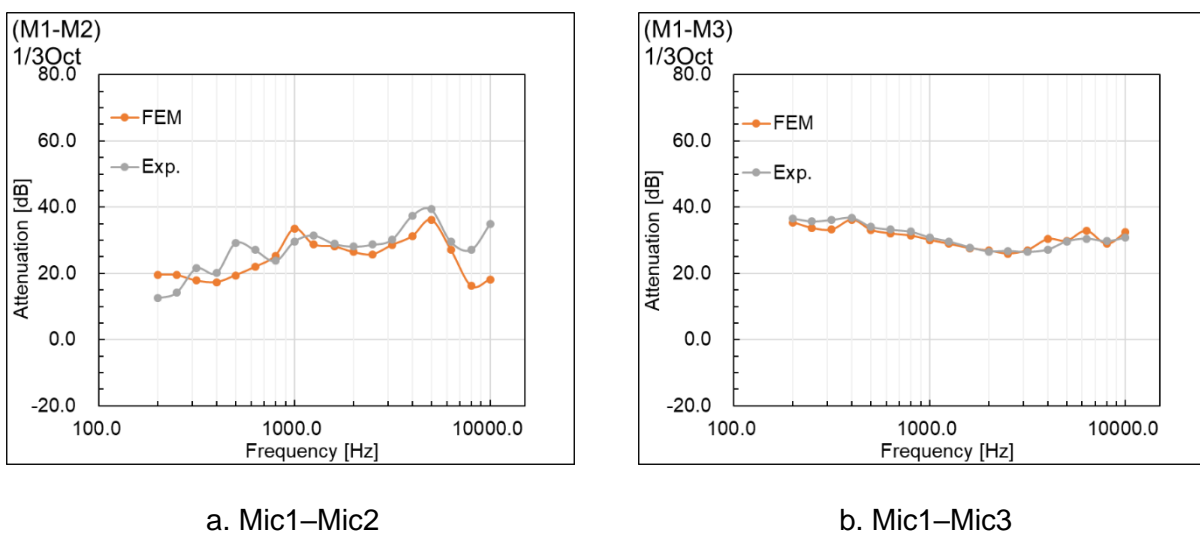
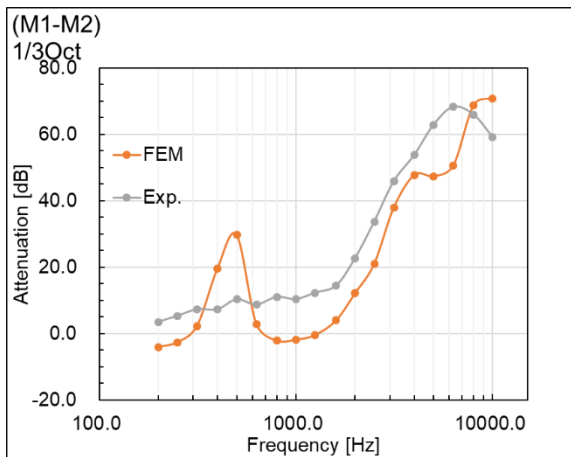
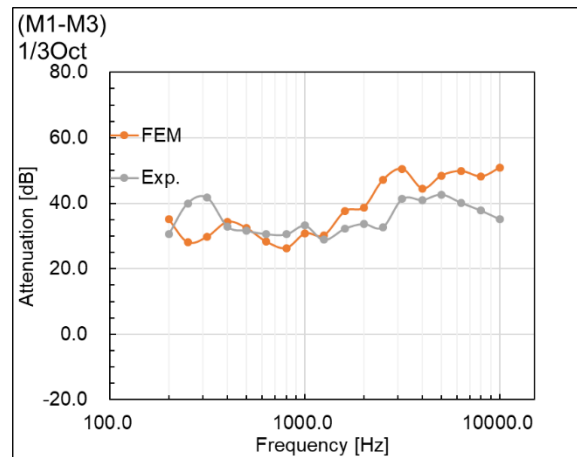


Fig. 4. Comparison of FEM and experimental results (Felt 2t).

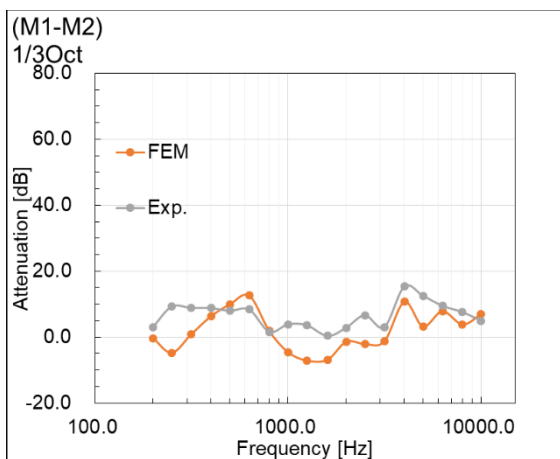


a. Mic1-Mic2

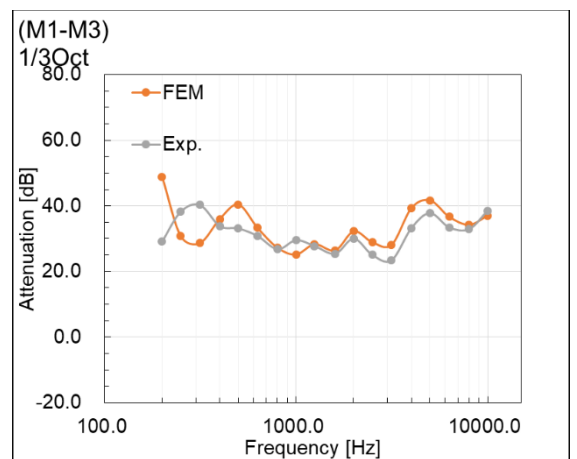


b. Mic1-Mic3

Fig. 5. Comparison of FEM and experimental results (Felt + film (out side)).

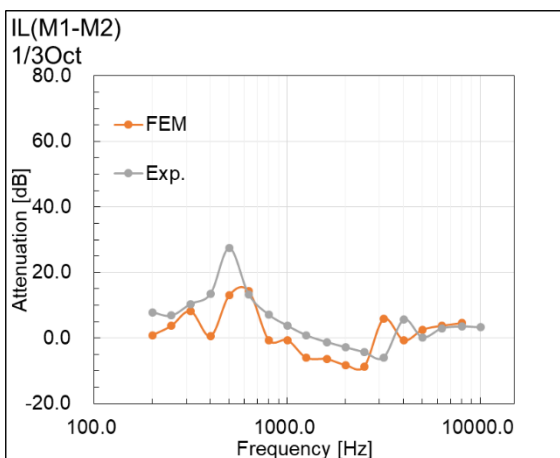


a. Mic1-Mic2

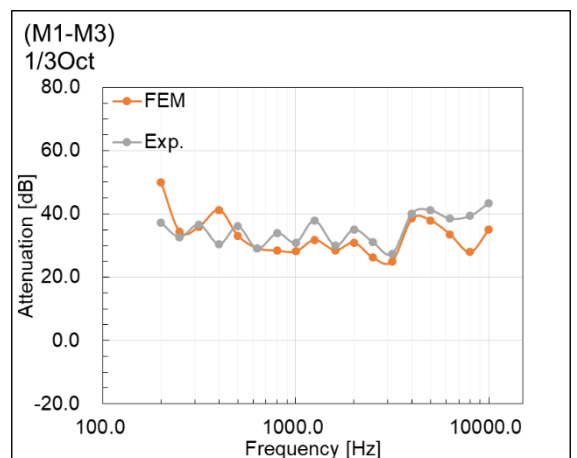


b. Mic1-Mic3

Fig. 6. Comparison of FEM and experimental results (Felt + film (in & out side)).



a. Mic1-Mic2



b. Mic1-Mic3

Fig. 7. Comparison of FEM and experimental results (PP).

4. Conclusion

We developed four types of test pieces for automobile air-conditioning ducts with PP resin, compressed felt, and films on the outside and both sides of the compressed felt. Two types of volume reduction were evaluated, one on the opposite side and the other on the outside from the entrance of the duct. At the duct inlet–exit, the compression felt test piece performed best up to 2500 Hz, whereas the test piece with film on the outside performed best above 2500 Hz. A type with a 0.05 mm thick PP film attached to the outside of a compressed felt with a basis weight of 1000 g/m² was able to improve insertion loss by 60 dB in the range of 5000 Hz to 10000 Hz compared to conventional resin ducts. Near the center of the duct inlet–outside, the difference between the four specifications was smaller than that of the duct inlet–outlet. However, the performance of the test piece with the film on the outside was slightly better than that of the conventional resin type. The calculated results of the FE model were able to roughly reproduce the experimental results. The weight of the test piece with film on the outside is about half that of the resin type; thus, sound performance could be improved while the weight could be simultaneously reduced. In the future, we intend to conduct parameter studies and study structures and material properties with better sound performance.

In the future, we plan to conduct parameter studies on the material properties of compressed felt and film to determine which material properties have the greatest effect on noise reduction.

References

- [1] H.J. Sabine, “The absorption of Noise in Ventilating Ducts”, *Journal of the Acoustical Society of America*, Vol.12, No.53, pp.53–57, 1940.
- [2] *Noise and vibration control*, L.L. Beranek, McGraw Hill, Inc (New York, USA), 1971.
- [3] *Propagation of sound in porous media*, J. F. Allard, N. Atalla, John Wiley & Sons (Chichester, UK), 2009.
- [4] Y. Kurosawa, J. Chengyao, T. Yamashita, T. Ozaki, N. Nakaizumi, Y. Fujita and M. Takahashi, “Vibro-acoustic analysis of sound absorbing duct using porous materials”, *Proceedings of Internoise2023* (Chiba, Japan), Aug 2023.